Spark plasma sintering of sol-gel derived 45S5 Bioglass®-ceramics: Mechanical properties and biocompatibility evaluation

Q.Z. Chen[1], J.L. Xu[2†], L.G. Yu[2], X.Y. Fang[1], K.A. Khor[2]

[1]Department of Materials Engineering, Monash University, Clayton, Victoria 3800, Australia

[2]School of Mechanical & Aerospace Engineering, Nanyang Technological University, 50 Nanyang Avenue, Singapore 639798, Singapore

Abstract

This work aims to find an efficient sintering technique and optimal sintering conditions of a novel sol-gel derived Bioglass®-ceramic powder so as to achieve much improved mechanical properties compared to conventional Bioglass®. To this end, the spark plasma sintering (SPS) technique was for the first time used to densify the sol-gel derived Bioglass®-ceramic powder. It was found that the sol-gel derived Bioglass®-ceramics sintered with the SPS technique at 950 °C for 15 min had a high Young's modulus value of ~110GPa, which was comparable to that of compact bone and significantly higher than the maximal value achieved by the conventional heat treatment. Moreover, the Bioglass®-ceramic compacts sintered with SPS released alkaline ions slowly and as a result, these highly densified Bioglass®-ceramics exhibited better cytocompatibility at the early stage of cell culture testing, compared to the conventional Bioglass®. Hence, the SPS technique is recommended to be used in the process of sol-gel derived Bioglass®-ceramics and its tissue engineering scaffolds.

Keywords*: Bioglass®, Sol-gel, Spark plasma sintering, Mechanical properties, Osteoblast.*

† Corresponding author Tel: 65 6790 4051 fax: 65 6792 4062 E-mail: jlxu@ntu.edu.sg

1. Introduction

To engineer bone tissues, which is hard and functions to support the body, the scaffold biomaterial must be strong and biodegradable such that it can temporarily replace the mechanical function of damaged bone until sufficient new bone tissue has formed. Unfortunately, mechanical strength and biodegradability, which are two essential requirements on bone tissue scaffolds, are antagonistic toward each other [1]. Compared to crystalline calcium phosphates which are virtually inert, amorphous bioactive glasses are biodegradable and tend to be mechanically fragile. Clinical investigation has shown that crystalline hydroxyapatite (HA) and related calcium phosphates are virtually inert, remaining within the body for as long as 6-7 years post implantation [2]. Actually among all bioceramics, Na_2O-containg bioactive glasses (e.g. 45S5 Bioglass®) are the only one that could simultaneously achieve both mechanical strength and satisfactory biodegradability through the formation of Na_2O-containg crystalline phase, $Na_2Ca_2Si_3O_9$ [3]. This mechanically capable crystalline phase can transform to a biodegradable, amorphous calcium phosphate at body temperature and in a biological environment (*in vitro*). This transformation couples the above two irreconcilable properties in one scaffold, and the transition temporal profile can be tailored to satisfy the requirement of bone tissue engineering [3]. Hence, 45S5 Bioglass® scaffolds offers a promise to go a long way towards the clinical application of bone tissue engineering.

Commercially produced 45S5 Bioglass® have been made by conventional glass powder manufacturing methods, i.e. melting and quenching. Meanwhile, increasing research efforts are being invested in fabrication of bioactive glasses using the sol-gel technique [4-9], which has many advantages over melting-quenching processes and is an extremely versatile process. Using the sol-gel process, ceramic or glass materials can be fabricated in a variety of forms, including ultra-fine spherical powders, thin film coatings, ceramic fibres, microporous

inorganic membranes, monolithic ceramics and glasses, or highly porous aerogel materials [5].

Most recently, Na_2O-containing glass-ceramics have been successfully synthesized by Chen et al, using a sol-gel technique in a water solution under the ambient conditions [8]. The sol-gel derived 45S5 glass-ceramic materials possess the major features of commercial Na_2O-containing bioactive materials, namely, the formation of crystalline phase $Na_2Ca_2Si_3O_9$ during sintering, decrease of the crystalline phase, and the extensive formation of amorphous bone-like apatite in a physiological environment. However, a drawback was also revealed that the sintering properties of the sol-gel derived 45S5 Bioglass®-ceramics powder was poor, compared to that of commercial 45S5 Bioglass® powder, and that the mechanical properties of the compact products of the sol-gel derived material was compromised. This forms the primary rationale of the present work: to explore alternative sintering techniques to process the sol-gel derived 45S5 Bioglass®-ceramics powder.

Advanced sintering methods, such as hot isostatic pressing [10] and spark plasma sintering (SPS), have proved advantageous over conventional pressureless sintering of bioceramics [11-14]. Materials of poor sintering properties, such as tungsten carbide (WC), have been successfully sintered, and a fracture toughness of 6 MPa $m^{1/2}$ being achieved with the SPS route [15]. In the SPS process, a high energy electric spark is discharged and the powder particle surfaces are more easily purified and activated than in conventional sintering process. The presence of spark plasma significantly enhances rapid densification to high densities from powder form [16]. Therefore, the objectives of this work are 1) to sinter sol-gel derived 45S5 Bioglass® compacts using either the SPS technique or conventional heat treatment, 2) to carry out a comparative investigation on the sintering kinetics and mechanical properties of 45S5 Bioglass®-ceramics produced by the above two methods, and 3) finally to investigate the biodegradation kinetics and biocompatibility of these 45S5 Bioglass®-ceramic materials.

2. Material and Methods

2.1. Material

The following chemicals were used as precursors for the synthesis of sol-gel 45S5 materials: tetraethyl orthosilicate (TEOS, Aldrich, 99%), triethyl phosphate (TEP, Eastman, 99.8%), sodium nitrite (Sigma-Aldrich, 99%) and calcium nitrate tetrahydrate (Sigma-Aldrich, 99%).

2.2. Methods

2.2.1. Sol-gel process and heat treatment

The recipe and processing flowchart have been reported previously [8]. In brief, the molar ratio of TEOS, TEP, $NaNO_3$ and $Ca(NO_3)_24H_2O$ was designed according to the molar ratio of SiO_2, P_2O_5, Na_2O and CaO in 45S5 Bioglass®. To achieve a clear sol, the molar ratio between water and the four precursor chemicals was set at 10. Each chemical was added reasonably slowly into the 0.25M HNO_3 aqueous solution at room temperature. Each compound in the sequence was added only when the previous solution became clear, and was then stirred for at least one hour. The resulting gel was dried at 60 and 200 °C for 72 and 40 h respectively, aged at 600°C for 5 h.

Pellets, which were prepared from the above aged 45S5 Bioglass® powder (~1.5g per pellet) under uniaxial pressure of 50 kPa, were divided into two groups. One group of pellets were sintered with the conventional heat treatment following the program of Fig. 1. The other group was sintered with the SPS technique at 600-950 °C for 15 min.

2.2.2. Characterisation

X-ray diffraction (XRD) of the powders and compacts was carried out using a Shimadzu 6000 Laboratory X-ray diffractometer utilising Cu K_α radiation at 40 kV and 30 mA with a graphite monochromator to collimate the X-rays. The step size and scan rate were fixed at 0.04^o and 1^o/min, respectively.

The distribution of particle size of the sol-gel derived powder was determined using laser diffraction analysis and analysed by Zeta Plus Particle sizing software Ver. 4.04, Brookhaven Instruments Corp. The particles were dispersed into deionised water for analysis. The morphology and composition of the powders and pellets were studied using scanning electron microscopy (SEM) JEOL 7001 at 15-20 keV. The SEM samples were gold coated to improve the conductivity and minimise electron charging in SEM.

The sintered densities of compacts were obtained by Archimedes' principle using de-ionized water as immersion medium. An ADA 210/L balance (Adam Co. Ltd., USA) equipped with density kit and analysis software was used.

2.2.3. Mechanical properties

The compressive strength of sintered materials was measured using an Instron 4204 tester at a crosshead speed of 0.5 mm/min, with a 1 kN load cell. The samples were rectangular in shape, with dimensions: 10mm in height and 5mm×5mm in cross-section. During compression testing, the load was applied until densification of the porous samples started to occur.

2.2.4. Measurement of pH values and ion concentrations

Samples (2g) of the materials to be tested were soaked in 10 ml of tissue culture medium in 15-ml cone tubes under standard cell culture conditions within a culture incubator (37ºC in humidified air containing 5% CO_2). Acidity was measured at 4, 12 and 24 hr by insertion of a pH glass electrode (Hanna Instruments, HI 1230B) attached to a pH meter (Hanna Instruments, HI 98185) into the solutions via an incubator access port, allowing the electrode to stabilize under incubation conditions for each reading.

The solutions used to analyse ion concentrations were prepared by soaking the materials of 2g in deionised water of 10 ml. Solutions were collected and transferred to new tubes at different intervals up to 2 days. All solutions were analyzed using ion chromatography. The

ICS-1000 (Dionex) ion chromatograph with attached autosampler was used for the analysis of sodium (Na^{+}) and calcium (Ca^{2+}) ions. The ICS – 2500 (Dionex) was used for the analysis of phosphate (PO_4^{3-}) and silicate (SiO_4^{2-}) anions. Before running a sample, the ion chromatography system is calibrated using a standard solution. By comparing the data obtained from a sample to that obtained from the known standard, sample ions can be identified and quantitated. The data collection system produces a chromatogram. The chromatography software converts each peak in the chromatogram to a sample convention and produces the results.

2.2.5. Cytocompatibility in vitro (ISO 10993-5)

Cytocompatibility study was performed according to the standard cytotoxicity assessment set by International Standardization Organization (ISO 10993-5). Extracts for tissue culture were prepared by placing 0.4 g of each material in 2 ml samples of cell culture medium (DMEM supplemented with 10% Fetal Calf Serum (FCS), 1% L-glutamine and 0.5% penicillin/streptomycin) for 24 hours at 37°C/5% CO_2 in culture incubator. Hydroxyapatite was used as the material control, and 2ml of cell culture medium alone was the negative control. Prior to exposure of cells to these extracts, human osteoblast-like cells (MG63, ATCC) were seeded in standard media at a density of approximately 2000 cells/well in 96 well tissue culture treated plates (Falcon, BD Bioscience, North Ryde, Australia), under standard incubation conditions (37ºC and 5% CO_2), with medium changed every second day. When the cell monolayers had reached 80 % confluence (at day 4), the medium in each well was entirely replaced with 0.2 ml of extract media samples (medium pre-exposed to material) or control media (material control = medium pre-exposed to PleuraSeal®; negative control = medium only). All cultures were then allowed to proceed for 2 days.

At the end of the incubation period, culture media were collected and the degree of cell death was determined by measurement of lactate dehydrogenase levels [17], as released into

the culture media ("RELEASED LDH"), using a commercial kit (Sigma-Aldrich TOX-7) as we have described previously [18]. Finally, each well containing living cells was filled with 0.2 ml fresh cell culture medium and cells were lysed using the solution TOX-7. These lysates were then used to determine the cellular LDH content, which equates to the number of living cells per well ("TOTAL LDH"). The overall LDH level was determined by measuring the absorbance of the supernatant from the centrifuged medium at 490nm (after subtraction for background absorbance at 690nm) using a multiwell plate format UV-vis spectrophotometer (Thermo Scientific). The absorbance results of LDH were converted to the number of cells according to a linear standard curve (not shown). Hence, cytotoxicity can be expressed as:

$$\text{Percentage of dead cells} = \frac{\text{RELEASED LDH}}{\text{RELEASED LDH} + \text{TOTALLDH}} \times 100 \qquad (1)$$

2.2.6.Cell proliferation: AlamarBlue™

Cell proliferation was assessed using a commercial AlamarBlue™ assay kit (Life Technologies). AlamarBlue™ is non-toxic to cells. The assay does not interrupt cell culture, allowing continuous measurement of cell proliferation kinetics. Hence, the AlamarBlue™ assay is appropriate to evaluate the long-term cytotoxicity of biomaterials due to biodegradation under physiological conditions. MG63 cells were seeded at 5000 cells/mL each well in a 48-well plate and cultured in the media with extracts. Incubated media in wells with neither cells nor testing materials extracts were used as negative controls. After culture for 48 hrs, 100 μL of AlamarBlue™ indicator was added to each well (except background controls) and incubated under culture conditions for 6 hrs. The media were then transferred to a new plate, followed by absorbance determination at wavelengths of 570 and 600 nm in a spectrophotometer (Thermo Scientific, Pathtech Australia).

The above procedures were repeated every 48 hrs until confluence was reached (between day 6-8). Cell proliferation was quantified by the percentage reduction of AlamarBlue. i.e.:

$$\%\ \text{Reduced AlamarBlue} = \frac{\varepsilon_{\text{OX}}(\lambda_2)A(\lambda_1) - \varepsilon_{\text{OX}}(\lambda_1)A(\lambda_2)}{\varepsilon_{\text{RED}}(\lambda_1)A^{-}(\lambda_2) - \varepsilon_{\text{RED}}(\lambda_2)A^{-}(\lambda_1)} \times 100\,, \qquad (2)$$

where $A(\lambda_1)$ and $A(\lambda_2)$ are the values of absorbance of test wells measured at a wavelength of λ_1 and λ_2, and $A^{-}(\lambda_1)$ and $A^{-}(\lambda_2)$ are the values of absorbance of negative control wells containing only media and AlamarBlue™ without cells. All values were blanked with the readings of background controls. The other parameters in Eq. (2) are as follows: $\varepsilon_{\text{OX}}(\lambda_1) = 80{,}586$, $\varepsilon_{\text{OX}}(\lambda_2) = 117{,}216$, $\varepsilon_{\text{RED}}(\lambda_1) = 155{,}677$ and $\varepsilon_{\text{RED}}(\lambda_2) = 14{,}652$.

2.2.7.Statistical analysis

All experiments were run with five samples per experimental group, and data are shown as mean ± standard error of the mean. One-way analysis of variance (ANOVA) with Tukey's post-hoc test as performed to analyse the statistical difference, and significance levels were set at a *p*-value of less than 0.05.

3. Results and discussion

3.1. Composition of the sol-gel derived 45S5 Bioglass®-ceramic powder

The composition of the sol-gel derived glass-ceramic powder was determined using EDX analysis in SEM JEOL 7001, as listed in Table 1, which is reasonably close to the nominal composition of 45S5 Bioglass® [19]. The results from particle sizing showed that 90% of the powders are in the range of 5-23 μm with a mean diameter ~ 7.6 μm. The $d_{0.1}$, $d_{0.5}$ and $d_{0.9}$ are 5.32, 8.60 and 17.6 μm, respectively.

3.2. Sintering kinetics of sol-gel derived 45S5 Bioglass®-ceramic pellets

A curve of relative density (i.e. $\frac{\rho}{\rho_{BG}}$, where ρ and $\rho_{BG} = 2.7\,g/cm^3$ are the densities of a sintered pellet and of a fully densified Bioglass® material [20]) against sintering conditions was determined, as shown in Fig. 2. The pellets, which were prepared from ~1.5g 45S5 Bioglass® powder under uniaxial pressure of 50 kPa, were sintered with the either SPS technique or conventional heat treatment. It was found that a maximum relative density, ~0.92 or 0.89, was achieved at 950 and 1200°C with the SPS technique and conventional heat treatment, respectively. Further raising the sintering temperature did not increase the density further. Hence, the SPS is more efficient than the conventional heat treatment.

3.3. Characterisation of sintered sol-gel derived 45S5 Bioglass®-ceramic pellets

It has been reported that a crystalline phase $Na_2Ca_2Si_3O_9$ forms in the sol-gel derived glass-ceramic powder sintered with the conventional heat treatment [8]. The XRD analysis of this work (Fig. 3) showed that this phase presented in the sol-gel derived Bioglass®-ceramics after sintering with the SPS technique at 600-950 °C for 15min.

SEM examination revealed many micropores in the Bioglass-ceramics after sintering with the conventional heat treatment at all conditions (Figs. 4a and c). Fine crystalline particles of $Na_2Ca_2Si_3O_9$ phase formed and distributed homogenously in the glass matrix after sintering at up to 1000°C for 2 hr (Fig. 4b). It should be mentioned that the maximal crystallinity is about 80% in 45S5 composition [3]. In most of the sintered materials, the amorphous phase forms a matrix to host the particles of the $Na_2Ca_2Si_3O_9$ crystalline phase (Figs. 4b, 5b and 5d). The percentage of crystalline phase in sintered 45S5 Bioglass® is about 80%, according to previous work [1]. However, sintering at excessively high temperature, 1100 and 1200°C for 2 hr for example, resulted in the segregation of glass phase, leaving bared crystalline particles with virtually no glass matrix (Fig. 4d). This inhomogeneous microstructure indicates that an over-sintering process occurred at the 1100-1200°C / 2 hr conditions.

In contrast to the materials sintered with the conventional heat treatment, much fewer micropores presented in the glass-ceramics that were sintered with the SPS technique (Figs. 5a and c), especially the one sintered at 950°C (Fig. 5c). Fine and homogenously distributed crystalline particles of $Na_2Ca_2Si_3O_9$ phase were populated in the glass matrix after SPS at 800 and 950°C (Figs. 5b and d). The presence of fewer microvoids and homogeneous microstructure of fine crystalline particles in the glass matrix produced much improved mechanical properties in the SPS processed materials, compared to those treated with the convention heating process, as discussed in the next section.

3.4. Mechanical properties

Fig. 6 demonstrates the mechanical properties of the 45S5 Bioglass®-ceramic materials after sintering with the SPS technique and conventional heat treatment. The mechanical properties increased with increasing sintering temperature. The maximal values of Young's modulus achieved by the conventional heat treatment was about 90 GPa on average, which was lower than the maximal Young's modulus (~110 GPa) achieved by the SPS technique at 950 °C (Fig. 6a). Moreover, the small standard deviation of mechanical properties of SPS samples indicates that their mechanical performance is reliable. In contrast, the conventional sintered compacts showed larger standard deviation due to the inhomogeneous structure, as manifested in Fig. 4.

Similarly, the ultimate compressive strength (UCS) of this material system was collectively higher after sintering with the SPS technique than with the convention heat treatment (Fig. 6b), with the maximal UCS being ~110 and ~98 MPa, respectively. However, the difference in the maximal UCS of the materials sintered by the two methods is insignificant ($p > 0.05$). It should be mentioned that the UCS of cortical bone is in the range of 50-150 MP [21-24]. Hence the sintered 45S5 Bioglass®-ceramics is comparable to the natural compact bone, in terms of mechanical properties.

Equally importantly, the mechanical reliability of the Bioglass®-ceramics was also improved by the SPS technique, as indicated by the scatterings (error bars) of the Young's moduli and UCS, which are significantly smaller in the materials sintered with the SPS technique than in those sintered with the conventional heat treatment (Fig. 6a and b). The mechanical properties shown in Fig. 6 are consistent with their microstructures shown in Figs. 4 and 5. The higher incidence of microvoids in the materials sintered with the convention heat treatment is most likely responsible for the poor mechanical performance (i.e. lower mean values of mechanical properties and larger scatterings of raw data), compared to those sintered with the SPS technique. Hence, we conclude that the SPS technique is an efficient sintering method, which can densify the sol-gel derived Bioglass-ceramics quickly, cheaply and reliably.

3.5. pH values of culture medium exposed to the Bioglass®-ceramics

The negative control was the media which was not in contact with any tested materials, and positive control was the media exposed to HA. Compared with the two control groups, the pH values of the media were increased when in contact with the Bioglass®-ceramic materials (Fig. 7), indicating that alkaline ions had been released. The change in pH values was considerably slower in the media soaked with relatively well sintered pellets, i.e. SPS at 800 and 950ºC and conventional heat treatment at 1000-1200ºC. It is apparent that the change in pH value, as well as the ion release (Fig. 8), was primarily controlled by the level of densification in these materials, as significant densification was observed with the materials sintered at these conditions (SPS at 800 and 950°C and conventional heat treatment at 1000-1200 °C), as indicated by the values of relatively density in Fig. 2, SEM examination (Figs. 4 and 5) and the mechanical properties in Fig. 6. It is likely that the surface area exposed to the medium was significantly reduced in these densified materials, because a porous sample has a larger surface area exposed to the surrounding liquid, resulting in faster ion release.

3.6. Ion Release into the deionised water from the Bioglass®-ceramics

There was no significant difference in the sodium ion concentrations after 24 hr soaking ($p > 0.05$) (Fig. 8). However, considerably higher sodium concentrations were detected in the first 24 hrs in the solutions soaked with the materials sintered at lower temperature, e.g. conventional heat treatment at 800°C (Fig. 8b) or SPS at 600°C (Fig. 8d), compared to those soaked with relatively well densified materials (Figs. 8a and c). This result is reasonably in agreement with the data of pH measurement (Fig. 7). The difference in the release of other ions, i.e. calcium (Ca^{2+}) ions, phosphate (PO_4^{3-}) and silicon (SiO_4^{2-}) anions, was insignificant between any two of the tested groups. The different time-release patterns among the samples were primarily due to the degree of densification of samples. Densified samples showed slow ion release kinetics at the early stage of soaking. Hence, it was concluded that the pH value of the medium was primarily affected by the release of sodium ions when exposed to the Bioglass®-ceramic materials.

3.7. Evaluation of cytocompatibility

The biocompatibility of melt-derived 45S5 Bioglass® has been evaluated previously, both *in vitro* and *in vivo* [25-27]. Given that the current 45S5 Bioglass®-ceramics was produced by a new process, it was necessary to evaluate the biocompatibility of the materials, using the cytocompatibility standard described by ISO 10993-5 which is required by the FDA. Hydroxyapatite was used as a positive control in this work. Medium containing the extracts of sintered powders was found to support proliferation of MG63 cells, and visual microscopic observation could identify no gross differences in cell proliferation at day 2 in the following six groups of samples: two controls, Bioglass®-ceramics sintered at 1000 and 1200 °C with the conventional heat treatment (Fig. 9) and materials sintered at 800 and 950°C with the SPS technique (Fig. 10c and d). The proportions of dead cells observed in MG63 cultures exposed to these sintered materials or HA were not significantly different ($p > 0.05$) (Fig. 11).

However, the cell growth was apparently slow at day 2 in the media containing the extracts of materials sintered with the SP technique at low temperature, i.e. 600 and 750°C (Fig. 10a and b), which was confirmed by the quantitative assessment (Fig. 11).

However, there was no significant difference in cell proliferation after day 2, as indicated by the quantitative assessment using the AlamarBlue™ technique (Fig. 12). It was revealed that the growth kinetics of MG63 cells were generally similar between media tested, with no significant difference seen between any two of the cellular growth kinetic curves ($p > 0.05$) at day 4 and 6. Further evaluation at extended time points is needed to verify the long-term safety and efficacy.

4. Conclusions

This work has explored the spark plasma sintering (SPS) of sol-gel derived 45S5 Bioglass®-ceramics. The SPS has been proved to be much more efficient than the conventional heat treatment for sintering the present sol-gel derived 45S5 Bioglass®-ceramics. The optimal SPS conditions were found to be around 950ºC for 15 min, which can improve mechanical properties of the sol-gel derived 45S5 Bioglass®-ceramics, compared to those sintered with the conventional heat treatment at above 1000ºC for 2 hr. This investigation also revealed that the Bioglass®-ceramics sintered at the optimal conditions released alkaline ions slowly, especially at the early stage of incubating, such that the change of pH value in the surrounding medium was mild. As a result, the well densified Bioglass®-ceramics exhibited better cytocompatibility at the early stage of cell culture, compared to the counterparts sintered at other conditions, although there was no significant difference from a long-term point of view. Hence, we recommend that SPS technique be used in the process of sol-gel derived Bioglass®-ceramics and its tissue engineering scaffolds.

References

[1] Chen QZ, Boccaccini AR. Coupling mechanical competence and bioresorbability in Bioglass (R)-derived tissue engineering scaffolds. Advanced Engineering Materials. 2006 Apr;8(4):285-9.

[2] Marcacci M, Kon E, Moukhachev V, Lavroukov A, Kutepov S, Quarto R, et al. Stem cells associated with macroporous bioceramics for long bone repair: 6- to 7-year outcome of a pilot clinical study. Tissue Engineering. 2007;13(5):947-55.

[3] Chen QZ, Thompson ID, Boccaccini AR. 45S5 Bioglass (R)-derived glass-ceramic scaffolds for bone tissue engineering. Biomaterials. 2006 Apr;27(11):2414-25.

[4] Li R, Clark AE, Hench LL. An investigation of bioative glass powders by sol-gel processing. Journal of Applied Biomaterials. 1991 Win;2(4):231-9.

[5] Hench LL. Sol-gel materials for bioceramic applications. Current Opinion in Solid State & Materials Science. 1997;2(5):604-10.

[6] Ramila A, Balas F, Vallet-Regi M. Synthesis routes for bioactive sol-gel glasses: Alkoxides versus nitrates. Chemistry of Materials. 2002;14(2):542-8.

[7] Jones JR. New trends in bioactive scaffolds: The importance of nanostructure. Journal of the European Ceramic Society. 2009;29(7):1275-81.

[8] Chen QZ, Li YA, Jin LY, Quinn JMW, Komesaroff PA. A new sol-gel process for producing Na2O-containing bioactive glass ceramics. Acta Biomaterialia. 2010 Oct;6(10):4143-53.

[9] Carta D, Pickup DM, Knowles JC, Smith ME, Newport RJ. Sol-gel synthesis of the P2O5-CaO-Na2O-SiO2 system as a novel bioresorbable glass. Journal of Materials Chemistry. 2005;15(21):2134-40.

[10] Wiegand C, Hipler UC. Polymer-based Biomaterials as Dressings for Chronic Stagnating Wounds. In: Heinze T, Janura M, Koschella A, editors. Utilization of Lignocellulosic Materials2010. p. 1-13.

[11] Takagi M, Mochida M, Uchida N, Saito K, Uematsu K. FILTER CAKE FORMING AND HOT ISOSTATIC PRESSING FOR TZP-DISPERSED HYDROXYAPATITE COMPOSITE. Journal of Materials Science-Materials in Medicine. 1992 May;3(3):199-203.

[12] Gu YW, Loh NH, Khor KA, Tor SB, Cheang P. Spark plasma sintering of hydroxyapatite powders. Biomaterials. 2002 Jan;23(1):37-43.

[13] Takahashi J, Kawano S, Shimada S, Kageyama K. Fabrication and electrical properties of Bi4Ti3O12 ceramics by spark plasma sintering. Japanese Journal of Applied Physics Part 1-Regular Papers Short Notes & Review Papers. 1999 Sep;38(9B):5493-6.

[14] Wu CT. Methods of improving mechanical and biomedical properties of Ca-Si-based ceramics and scaffolds. Expert Review of Medical Devices. 2009 May;6(3):237-41.

[15] Omori M. Sintering, consolidation, reaction and crystal growth by the spark plasma system (SPS). Materials Science and Engineering a-Structural Materials Properties Microstructure and Processing. 2000 Aug;287(2):183-8.

[16] Xu JL, Khor KA. Chemical analysis of silica doped hydroxyapatite biomaterials consolidated by a spark plasma sintering method. J Inorg Biochem. 2007(101):187-95.

[17] Schildhauer TA, Gekle CJE, Muhr G. Biomaterials in the skeletal system. Chirurg. 1999 Aug;70(8):888-96.

[18] Berchtold MW, Brinkmeier H, Muntener M. Calcium Ion in Skeletal Muscle: Its Crucial Role for Muscle Function, Plasticity, and Disease. Physiol Rev. 2000 July 1, 2000;80(3):1215-65.

[19] Clupper DC, Gough JE, Embanga PM, Notingher L, Hench LL, Hall MM. J Mat Sci: mat med. 2004 (15):803-8.

[20] Hench LL, Wilson J. An Introduction to Bioceramics. 2 ed. London: Word Scientific; 1999.

[21] Nalla RK, Kinney JH, Ritchie RO. Mechanistic fracture criteria for the failure of human cortical bone. Nature Materials. 2003 Mar;2(3):164-8.

[22] Zioupos P, Currey JD. Changes in the stiffness, strength, and toughness of human cortical bone with age. Bone. 1998 Jan;22(1):57-66.

[23] Keaveny TM, Hayes WC. Mechanical properties of cortical and trabecular bone. In: Hall BK, editor. Bone A Treatise, Vol 7:Bone Growth. Boca Raton, FL: CRC Press; 1993. p. 285-344.

[24] Moore WR, Graves SE, Bain GI. Synthetic bone graft substitutes. Australian and New Zealand Journal of Surgery. 2001 Jun;71(6):354-61.

[25] Saravanapavan P, Selvakumaran J, Hench LL. Indirect cytotoxicity evaluation of soluble silica, calcium, phosphate silver ions. Bioceramics 16. 2004;254-2:785-8.

[26] Saravanapavan P, Jones JR, Verrier S, Beilby R, Shirtliff VJ, Hench LL, et al. Binary CaO-SiO2 gel-glasses for biomedical applications. Bio-Medical Materials and Engineering. 2004;14(4):467-86.

[27] Stanley HR, Hall MB, Clark AE, King CJ, Hench LL, Berte JJ. Using 45S5 bioglass cones as endosseous ridge maintenance implants to prevent alveolar ridge resorption: A 5-year evaluation. International Journal of Oral & Maxillofacial Implants. 1997;12(1):95-105.

List of Table

List of Figures

treatment at 1200 and 800°C for 2 hr, respectively; (c)-(d) sintered with the spark plasma technique at 950 and 600°C for 15 min, respectively.

Fig. 9 Typical morphology of MG63 cells cultured for 2 days in (a) the standard culture medium, (b) the extractant medium of hydroxyapatite, (c)-(d) the extractant medium of sol-gel derived Bioglass®-ceramics sintered with the conventional heat treatment at 1000 and 1200°C, respectively. Magnificence of the images is the same.

Fig. 10 Typical morphology of SNL cells cultured for 2 days in the extractant medium of sol-gel derived Bioglass®-ceramics sintered with the spark plasma technique at (a) 600°C, (b) 750°C, (c) 800°C, and (d) 950°C. Magnificence of the four images is the same.

Fig. 11 Cytotoxicity of the test materials using MG63 cells, detected by measuring the release of lactate dehydrogenase (LDH) into medium containing the extracted substances during 2 days culture. Medium with hydroxyapatite extracts served as the positive control. Sol–gel derived Bioglass®-ceramics were sintered with either the conventional heat treatment or spark plasma sintering (SPS) technique. No significant differences were found in the percentage of dead cells between any two of the following six groups ($p > 0.05$): two controls and sol-gel derived Bioglass® heat treated at 1000 and 1200°C or SP sintered at 800and 950°C. However, the percentages of dead cells were significantly higher in the Bioglass® sintered with the SPS technique at 600and 750°C ($p < 0.05$), compared to the rest of tested groups. n = 5.

Fig. 12 MG63 cell proliferation kinetics measured by the AlamarBlue™ technique. The initial plating density was 5000 cells ml^{-1} in each well of a 48-well plate (n = 5). Medium with the hydroxyapatite extract were the positive control. Sol–gel derived Bioglass®-ceramics were sintered with either the conventional heat treatment or spark plasma sintering (SPS) technique. The differences between any two groups were not

significant ($p > 0.05$) on days 4–6. The cell growth was apparently lower on day 2 in the extractant media of materials sintered with SPS technique at 600 and 750°C, compared to the rest of groups.

Bioglass®

	Sol-gel derived Bioglass®-ceramics mol %	Nominal Bioglass® mol%
Si	47.22	46.1
Na	45.96	48.8
Ca	27.03	26.9
P	5.54	5.0

Table 1

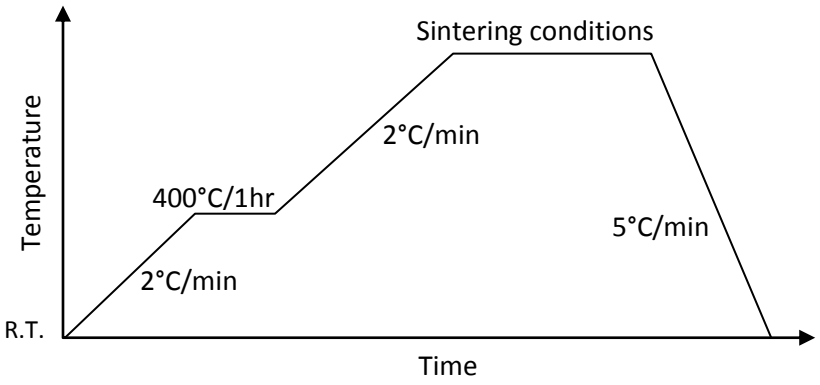
Sintering conditions
2°C/min
400°C/1hr
5°C/min
2°C/min
Temperature
R.T.
Time

Fig. 1

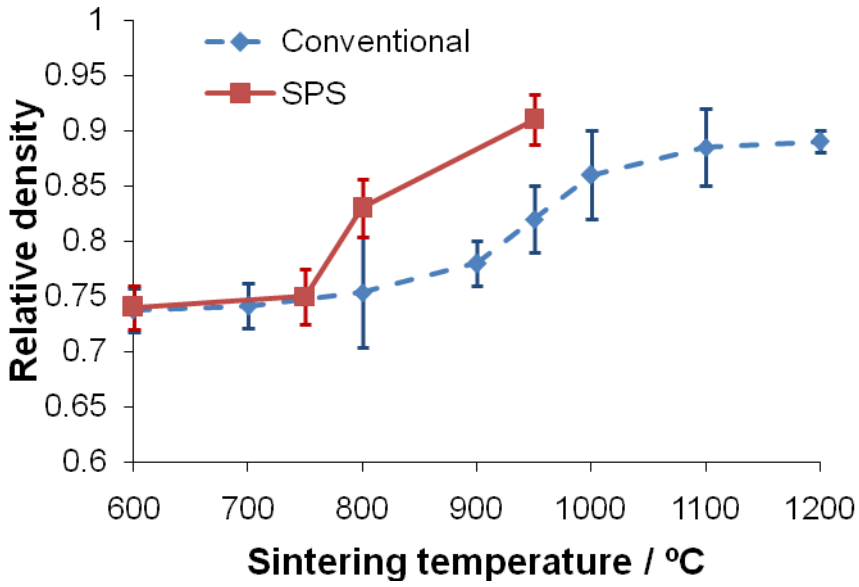
Conventional
SPS
Relative density
1
0.95
0.9
0.85
0.8
0.75
0.7
0.65
0.6
600
700
800
900
1000
1100
1200
Sintering temperature / ºC

Fig. 2

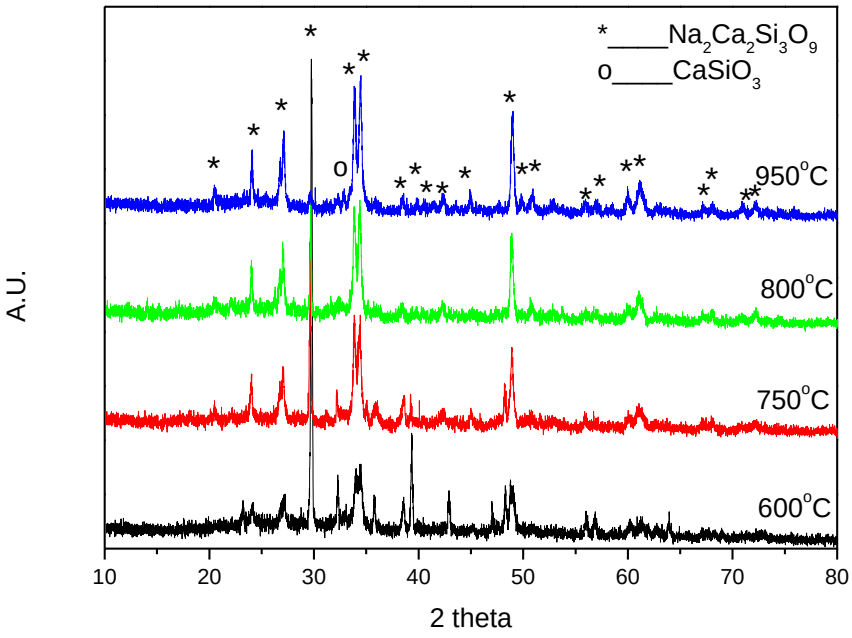
*____Na2Ca2Si3O9
o____CaSiO3
950°C
800°C
750°C
600°C
A.U.
2 theta
10
20
30
40
50
60
70
80

Fig. 3

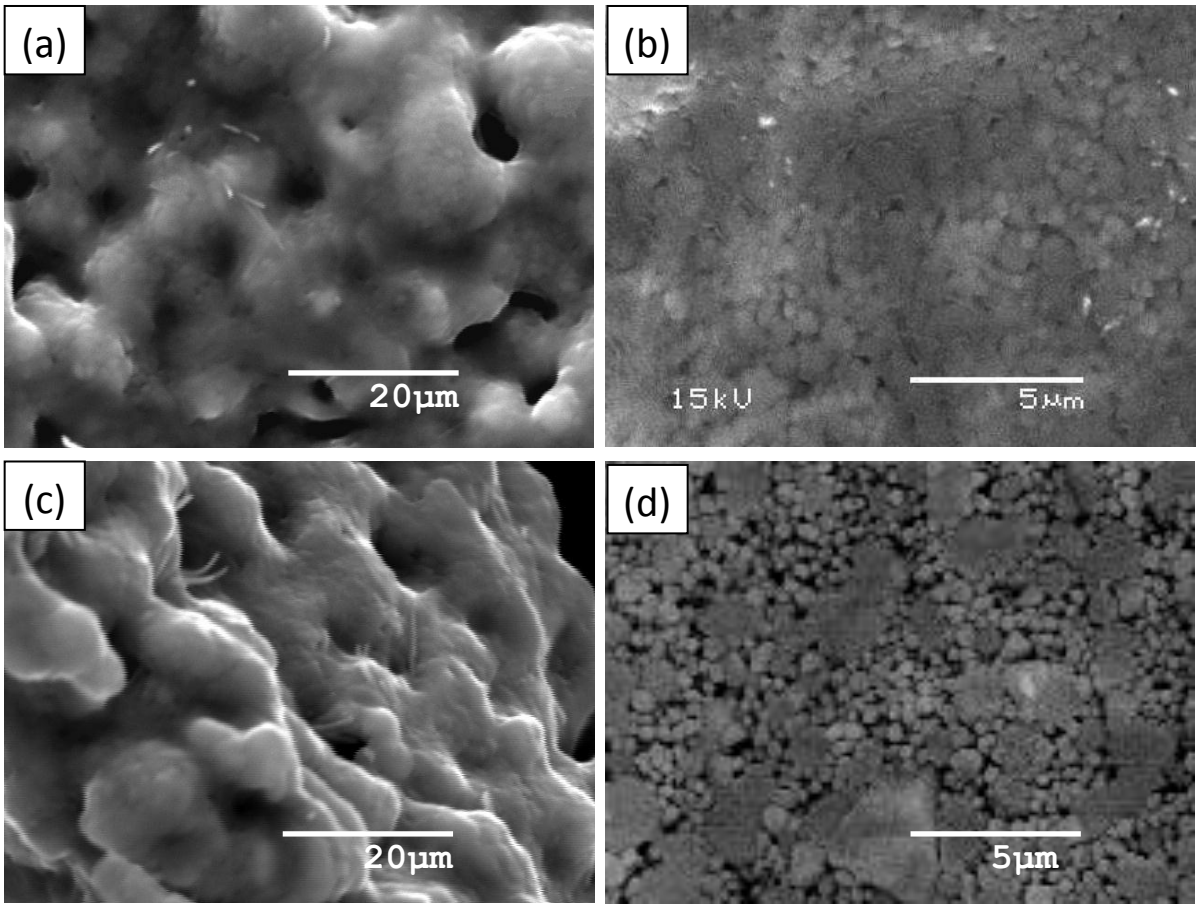

Fig. 4

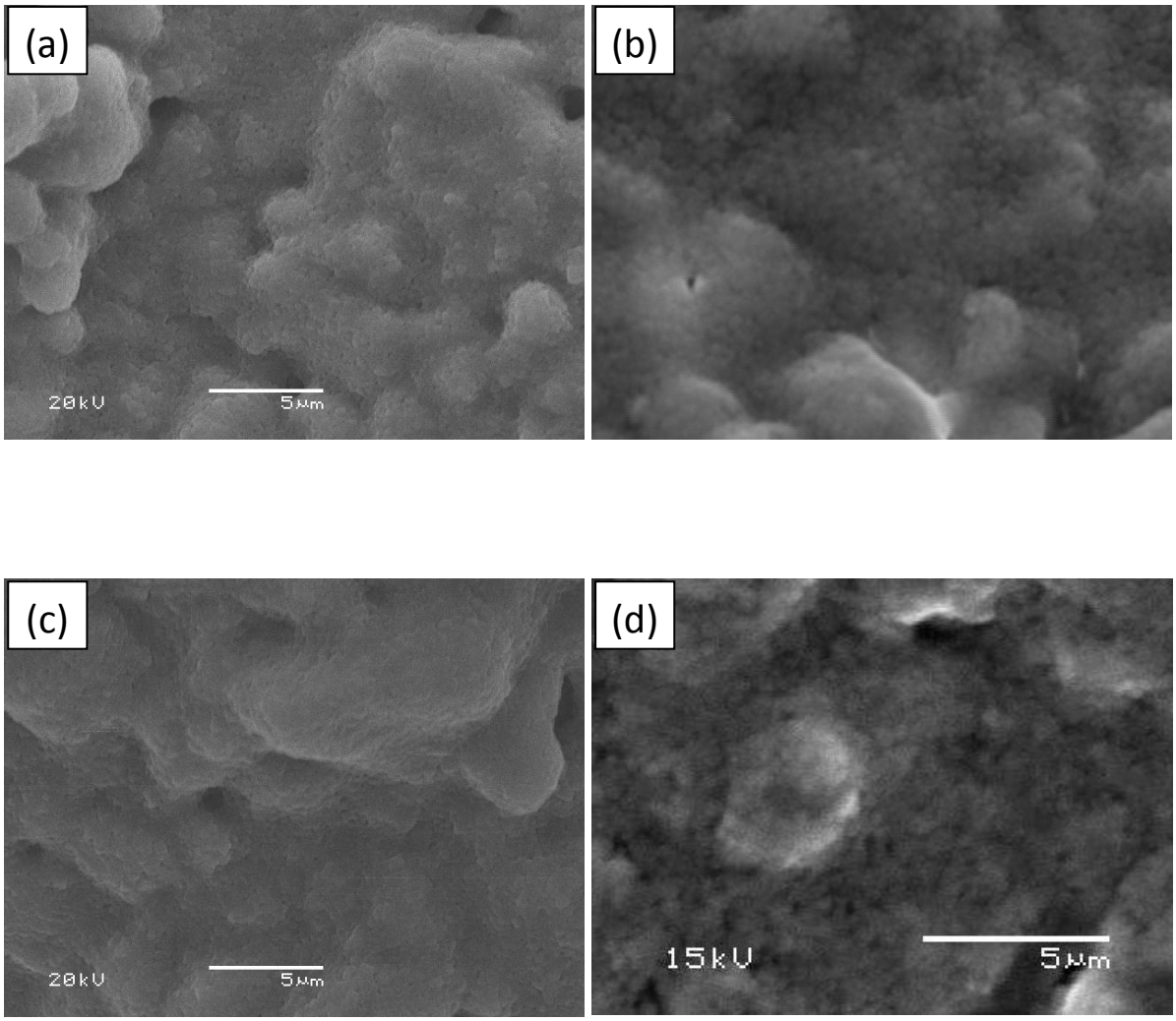

Fig. 5

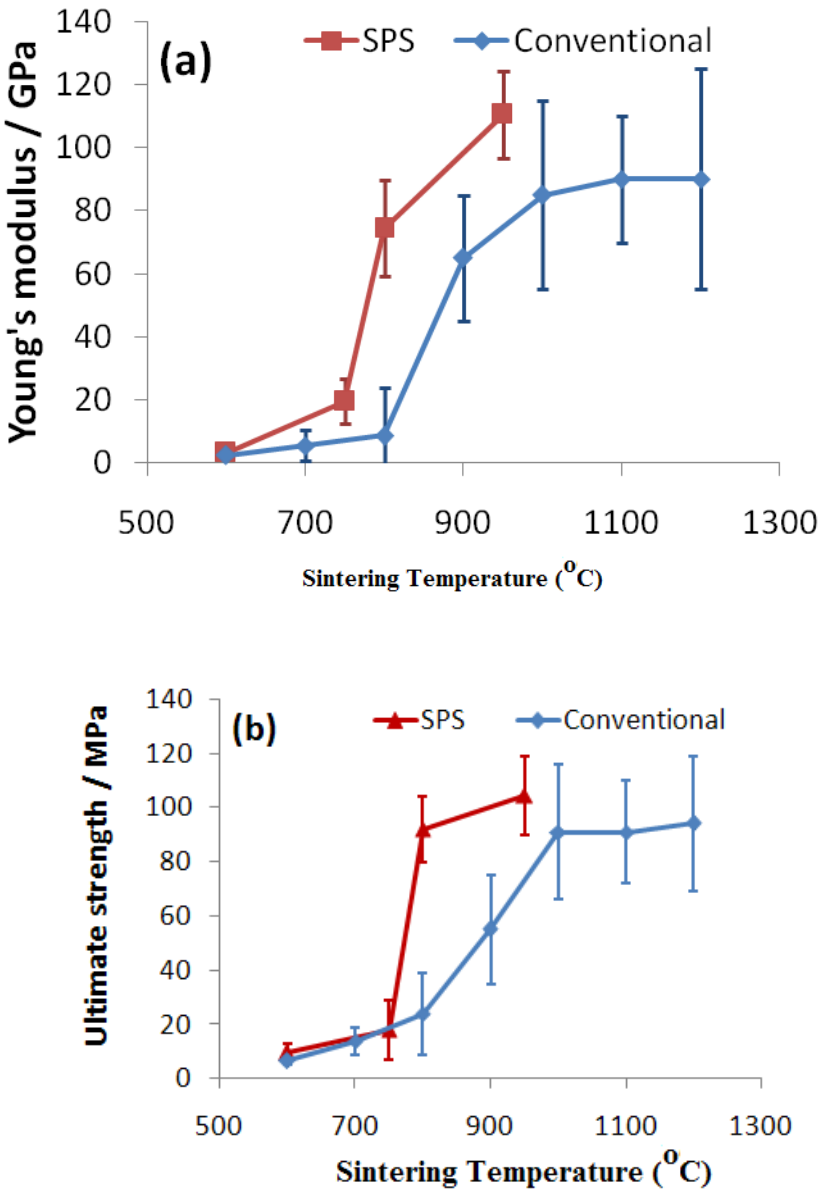
(a)
SPS
Conventional
Young's modulus / GPa
140
120
100
80
60
40
20
0
500
700
900
1100
1300
Sintering Temperature (°C)
(b)
SPS
Conventional
Ultimate strength / MPa
140
120
100
80
60
40
20
0
500
700
900
1100
1300
Sintering Temperature (°C)

Fig. 6

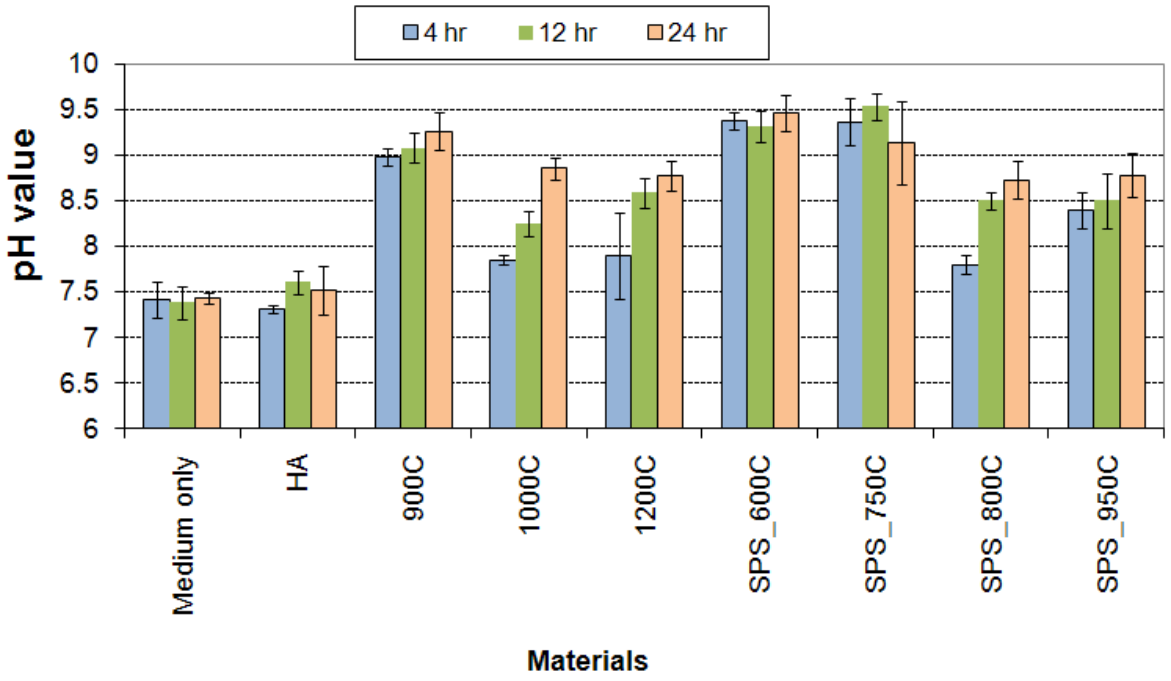
4 hr
12 hr
24 hr
pH value
10
9.5
9
8.5
8
7.5
7
6.5
6
Medium only
HA
900C
1000C
1200C
SPS_600C
SPS_750C
SPS_800C
SPS_950C
Materials

Fig. 7

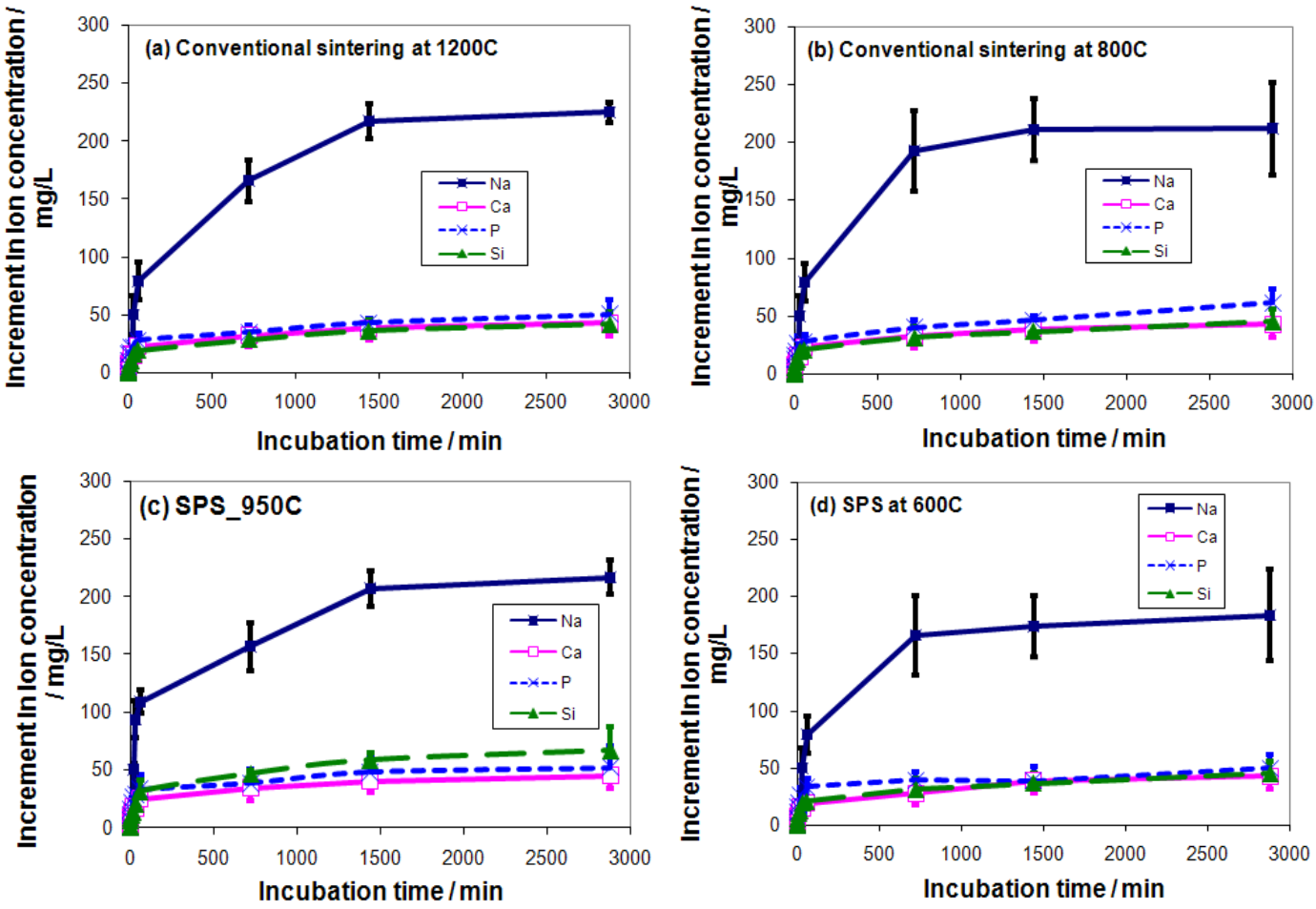
(a) Conventional sintering at 1200C
(b) Conventional sintering at 800C
(c) SPS_950C
(d) SPS at 600C
Increment In Ion concentration / mg/L
Incubation time / min
Na
Ca
P
Si
0
50
100
150
200
250
300
0
500
1000
1500
2000
2500
3000

Fig. 8

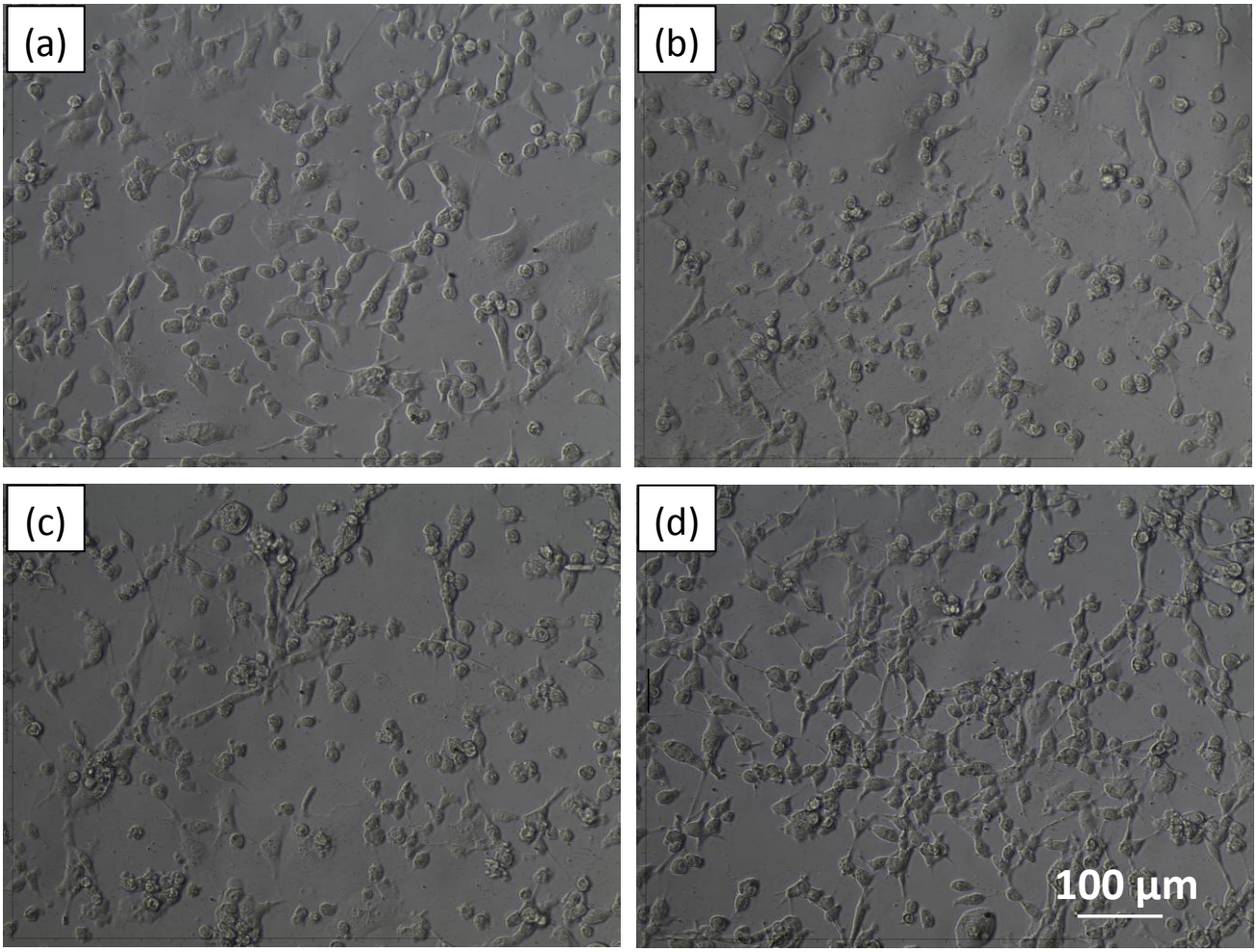

Fig. 9

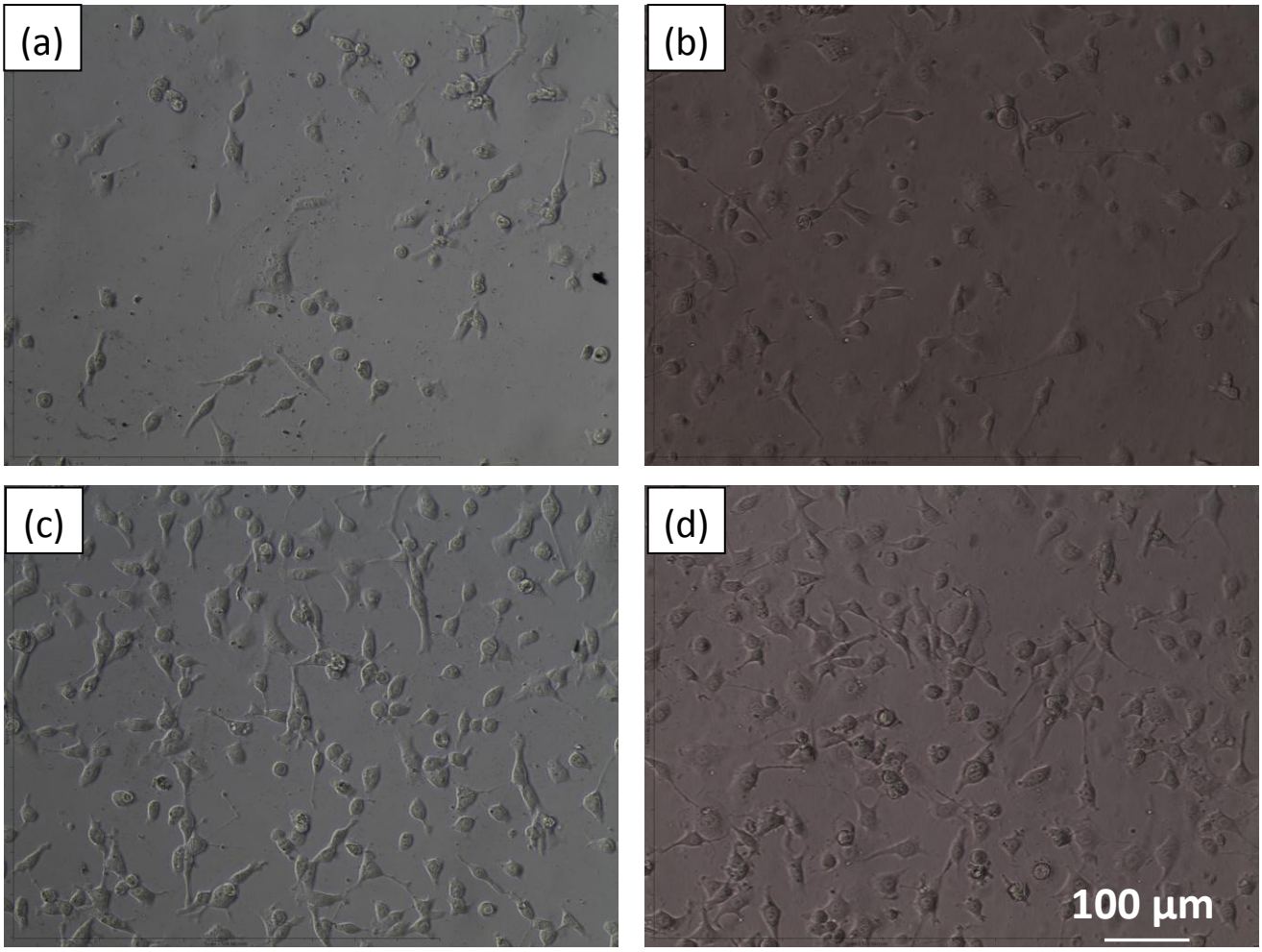

Fig. 10

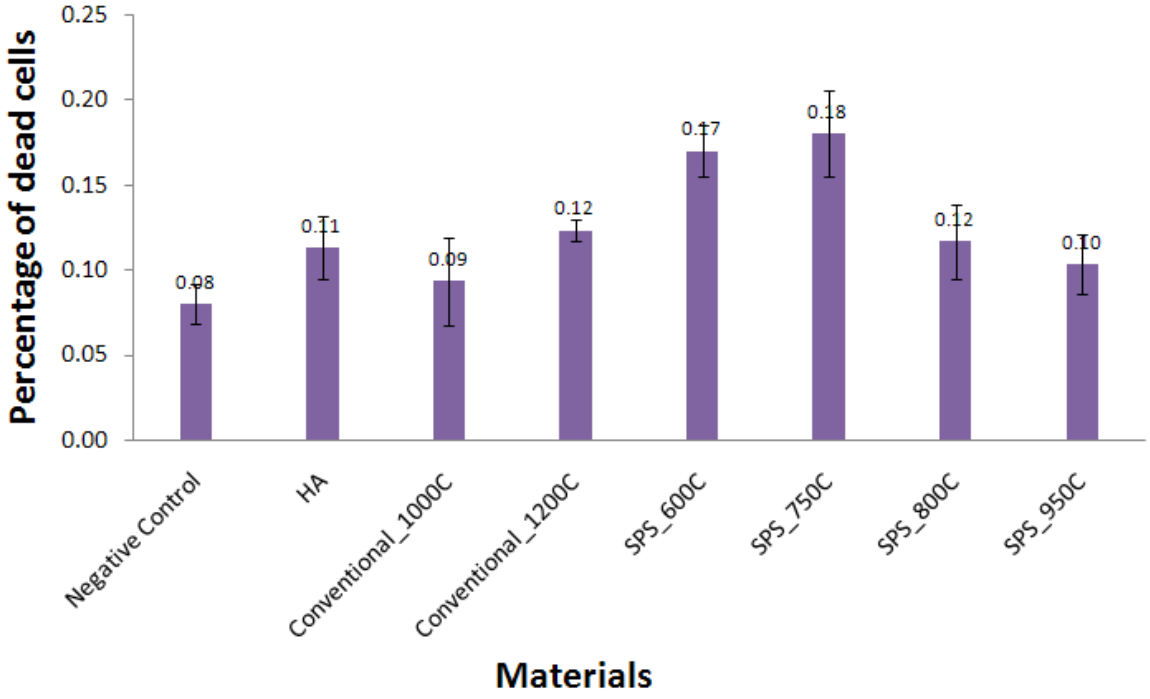
Percentage of dead cells
0.25
0.20
0.15
0.10
0.05
0.00
0.08
0.11
0.09
0.12
0.17
0.18
0.12
0.10
Negative Control
HA
Conventional_1000C
Conventional_1200C
SPS_600C
SPS_750C
SPS_800C
SPS_950C
Materials

Fig. 11

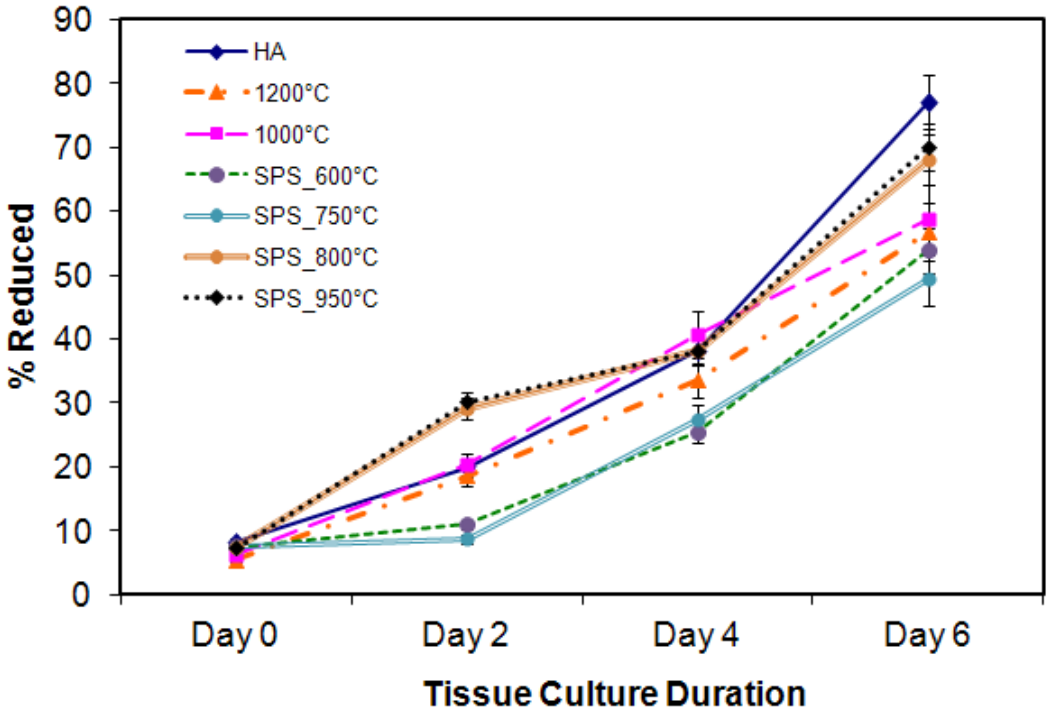
90
80
70
60
50
40
30
20
10
0
% Reduced
HA
1200°C
1000°C
SPS_600°C
SPS_750°C
SPS_800°C
SPS_950°C
Day 0
Day 2
Day 4
Day 6
Tissue Culture Duration

Fig. 12